Gómez-de la Cruz, F. J., Palomar-Carnicero, J. M., Hernández-Escobedo, Q., & Cruz-Peragón, F. (2021). Experimental studies on mass transfer during convective drying of spent coffee grounds generated in the soluble coffee industry. *Journal of Thermal Analysis and Calorimetry*, *145*(1), 97-107.

https://doi.org/10.1007/s10973-020-09600-3

Experimental studies on mass transfer during convective drying of spent coffee grounds generated in the soluble coffee industry.

Authors.

Francisco J. Gómez-de la Cruz[1*] (http://orcid.org/0000-0002-0206-832X), José M. Palomar-Carnicero[1](http://orcid.org/0000-0002-8003-1223), Quetzalcoatl Hernández-Escobedo, Fernando Cruz-Peragón[1].

[1]Dep. of Mechanical and Mining Engineering, Escuela Politécnica Superior de Jaén, University of Jaén, Campus Las Lagunillas s/n, 23071, Jaén (Spain).

*Corresponding author: Tel.: +34 953213002; Fax: +34 953212870; E-mail address: fjgomez@ujaen.es

Abstract.

Drying is a very important stage in the treatment of spent coffee grounds destined to biofuels production. The mass transfer during the convective drying of spent coffee grounds generated in the soluble coffee industry (SCG-SCI) is analyzed. An experimental design from sixteen isothermal drying experiments for different sample thicknesses (5mm, 10mm, 15mm and 20mm) and drying air temperatures (100ºC, 150ºC, 200ºC and 250ºC) using a drying air velocity of 1m/s was proposed. Drying

times, drying rates and effective diffusivity coefficients were obtained. Drying curves were fitted with the main mathematical model proposed in the literature and drying rates were studied from the moisture ratio and the drying air temperature. Constant and time-dependence effective diffusivity were evaluated using polynomial surface models. Drying times range between 18 minutes (test at 5 mm and 250ºC) and 3 hours (test at 20 mm and 100ºC). Drying rate and effective diffusivity values were found between 0.0000226 and 0.001722 s^{-1} and $1.79 \cdot 10^{-9}$ and $29.1 \cdot 10^{-9}$ m^2/s, respectively. The main differences between these experiments and those carried out by the same authors about the drying of spent coffee grounds obtained in the services sector (SCG-SS) were studied and analyzed.

Keywords: Biofuels; Drying; Drying rate; Effective diffusivity; Mathematical modeling; Spent coffee grounds.

Article Highlights.

-Mass transfer in the drying of SCG-SCI was studied.

-Drying curves, drying rate and effective diffusivity coefficients were obtained.

-In drying tests performed above at 200ºC, the samples experimented the release of volatile particles and combustion.

-SCG-SCI samples did not show shrinkage due mainly to their granulometry.

-Drying of SCG-SCI is more effective that drying of SCG-SS due to their particle size.

Nomenclature

$a_0, a_1, a_2, a_3, a_4, a_5, a_6, a_7, a_8$	Coefficients of the polynomial surface model
$a, b, c, d, e, f, k, k_0, k_1, n$	Coefficients of the thin-layer drying kinetics mathematical model
d_p	Particle size (mm)
D_{eff}	Effective diffusivity ($m^2 \cdot s^{-1}$)
DR	Drying rate (s^{-1})
Fo	Fourier number
L	Thickness of the slab (m)
N	Number of data
R^2	Coefficient of determination
RMSE	Root mean square error
SCG-SCI	Spent coffee grounds generated in the soluble coffee industry
SCG-SS	Spent coffee grounds generated in the service sector
t	Time (s)
T	Temperature (ºC, K)
v	Velocity ($m \cdot s^{-1}$)
x	Spatial dimension of mass transport (m)
X_e	Equilibrium moisture content (kg moisture/kg dry matter)
X_0	Initial moisture content (kg moisture/kg dry matter)
X_t	Moisture content at time t (kg moisture/kg dry matter)
XR	Dimensionless moisture ratio

1. Introduction

Coffee is one of the most popular beverages in the world. This product is the second largest traded commodity surpassed only by the petroleum. The annual average production of coffee is 8 million tons being the largest producers Brazil, Vietnam and Indonesia with a production of 35 %, 15.2 % and 8.8 %, respectively [1]. Spent coffee grounds are wastes obtained in the soluble coffee industry (henceforth SCG-SCI) and the service sector like cafeterias, restaurant, capsules… (henceforth SCG-SS). Large amounts of this by-product are produced as a result of the brewing process. Due to their high organic material content and the presence of compounds such as caffeine, tannins, and polyphenols, which can have negative effects on the environment and result in the release of greenhouse gases into the atmosphere, the disposal of these spent coffee grounds should be properly managed [2]. At present, spent coffee grounds are being used as fertilizers, animal feed, horticultural production, activated carbons and biochar [3]. Other applications of these wastes include their use as "green iron catalyst" in the Fenton's chemistry [4], the manufacture of Eco-fired clay bricks [5] and the production of nanocomposites [6].

Spent coffee grounds emerge as one of the bioresources most important and abundant in the world destined for green energy generation. Recently in Japan, the Fukushima nuclear disaster has promoted the use of spent coffee grounds for generating thermal and electrical energy. Furthermore, this waste is the main energy source in the own soluble coffee industry. Four types of biofuels can be obtained from them: biodiesel, bioethanol, bio-oil and fuel pellet [7]. Spent coffee grounds contain around 15% of oil. The oil extracted can be further converted into biodiesel using transesterification methods. The biodiesel extracted from spent coffee grounds has better stability than biodiesel from other sources due to its high antioxidant content [8-

10]. Other biofuels can be obtained from defatted solid wastes like bio-oil (slow pyrolysis) and bioethanol (fermentation). The leftover solid wastes are intended for the production of fuel pellet with a significant net calorific value of 25,240 $kJ \cdot kg^{-1}$ [11].

In the soluble coffee industry, spent coffee grounds present moisture contents around 85 % - 90 % (wet basis) [12]. In this sense, a first stage, before the drying process, consists of mechanical pressing, which reduces moisture to similar values as those used in the present study (60 % - 62 %) [13]. With these moisture content values, drying of these wastes until their equilibrium moisture content is a fundamental step to produce biofuels [14-16]. Even, when the spent coffee grounds are directly used as fuel pellet, drying improves their energy characteristics as biofuel increasing the combustion yield and avoiding condensation problems in boilers [17-19]. Moreover, drying minimizes the storage, packing and transport costs [20].

To study the drying of spent coffee grounds is very important to analyze the drying curves, the drying rate curves and mainly the effective diffusivity in each experimental test. Furthermore, it is clear that diffusion is not the only phenomenon that occurs during drying of agricultural and biomass products, other important phenomena such as capillary movements and sequential flow of evaporation-condensation are manifested [21]. In this sense, effective diffusivity, defined as an overall mass transport property of moisture, can be used as a measure of moisture rate, irrespective of the mechanism really involved [22, 23]. Correa et al. (2014) studied the drying of spent coffee grounds in a cyclonic dryer in a range of temperatures between 59ºC and 271ºC for different mass flow rate of air [13]. Gómez-de la Cruz et al. (2015) studied the drying kinetics of spent coffee grounds generated in the services sector in a convective dryer for different drying air temperatures and sample thicknesses [24]. Efthymiopoulos et al. (2019)

investigated the reduction of moisture content in spent coffee grounds by mechanical pressing used as alternative to thermal drying for purposes of solvents extraction [12]. So far, there are no works that have studied the mass transfer and diffusion coefficients during drying of spent coffee grounds obtained in the soluble coffee industry.

This work presents an exhaustive experimental study on the mass transfer from the analysis of drying curves, drying rates curves and effective diffusivity coefficients during drying of industrial coffee wastes. For that, a design of experiments based on the main parameters (and values) that influence in their drying on an industrial scale, sample thicknesses and air temperatures, has been taken into account. The calculation both the drying rates and the effective diffusivities are essential for analyzing the Fick's second law of diffusion equation in later numerical calculations and simulations and for enhancing the design of convective dryers like, for example, conveyor belt dryers or tray dryers widely used in the soluble coffee industry [25, 26]. Along with improving the design, the main objective is to optimize the drying efficiency in these dryers from the values obtained of these important variables, which until now are unknown. Furthermore, the results achieved are compared with those obtained in the drying of SCG-SS highlighting mainly the drying times, the drying rates and the effective diffusivities and the release of volatile matter and the combustion phenomenon in the samples [24]. The findings are presented and commented.

2. Materials and methods.

2.1 Materials

SCG-SCI samples were supplied by a company dealing on soluble coffee industry located in the northern region of Spain. Samples were received in July 2018 and immediately were frozen. Before carrying out drying experiments, several samples were unfrozen and dried in an oven (Memmert GmbH + Co.KG, SNB 167 Model 100, Germany) at 105 ºC for 24 hours to find out the initial moisture content, according to the norm CEN/TS 14774-1:2004. This procedure was performed in triplicate and an average value of initial moisture content of 61.1 ± 0.5% (wet basis) was found. Equilibrium moisture content was calculated by the same procedure in 8.5 ± 0.5% (wet basis) when the surrounding air conditions had a room temperature of 20 ºC and a relative humidity of 50 %. A quantity of waste was screened to get the particle size distribution by a vibratory screen (Restch, Mod. Vibro). The results showed the following granulometric composition taking into account the particle size (d_p) in mm: $d_p < 0.1$ (1.34%), $0.1 < d_p < 0.2$ (9.46%), $0.2 < d_p < 0.32$ (11.19%), $0.32 < d_p < 1.25$ (38.68%), $1.25 < d_p < 1.6$ (16.9%), $1.6 < d_p < 2.5$ (12.4%) and $d_p > 2.5$ (10.03%). Fig. 1 shows the granulometric distribution of the SCG-SCI samples studied.

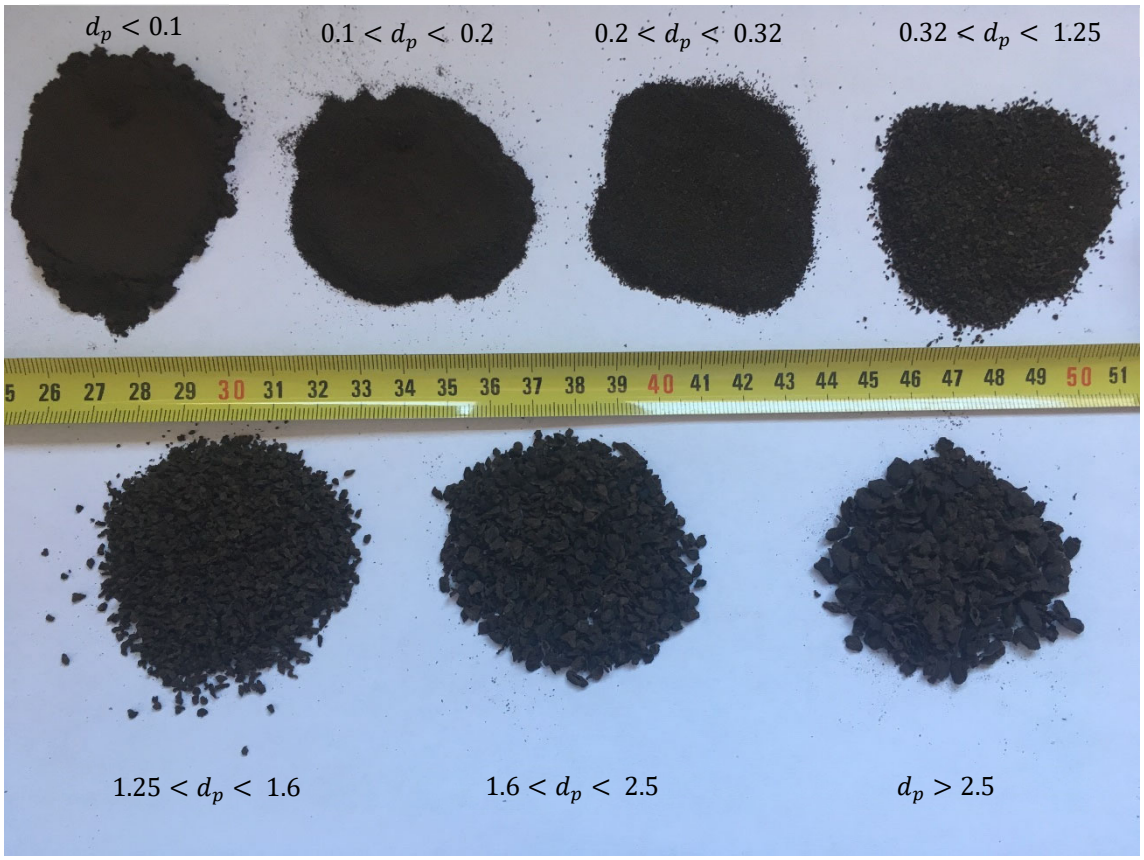

Figure 1. Classification according to particle size of spent coffee grounds obtained in the soluble coffee industry.

2.2 Drying equipment and procedure.

Drying experiments were carried out in a drying chamber described previously by Casanova-Peláez et al. (2015) [20] (Fig. 2). The dryer mainly consists of a centrifugal fan to supply the air with a maximum flow of 475 $m^3 \cdot h^{-1}$, a set of electrical resistances with a power range of up to 45 kW, a 2 m length tunnel with thermal insulation and a square section of 0.15 m, and a PID (Proportional-Integral-Derivative) controller which controls the drying air temperature near the sample measured with a PT100 sensor.

SCG-SCI samples were dried in a rectangular basket of 100 mm of width and 150 mm of length which was placed over a precision balance (Blauscal AH1200) with an error of ± 0.01 g. The balance was connected to a personal computer and the moisture loss was recorded in each second along drying in computer files.

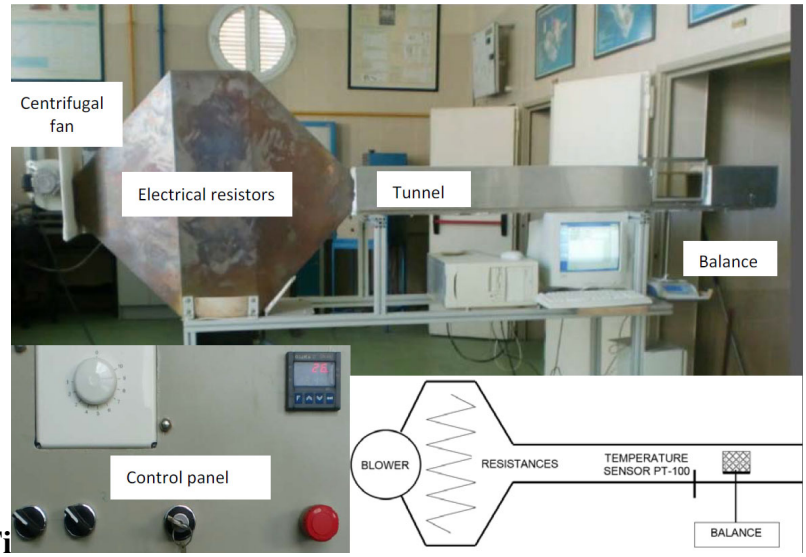

Fi

Figure 2. Drying equipment and scheme.

Drying of these wastes was studied from sixteen isothermal drying tests. For each of the sample thicknesses: 5, 10, 15 and 20 mm, four tests with constant drying air temperatures of 100, 150, 200 and 250 ºC were carried out. The design of experiments takes into account the drying conditions in typical drying equipment such as tray dryers and conveyor belt dryers widely used in this type of industries. All drying experiments were performed in triplicate. The drying air velocity was fixed at 1 ± 0.1 $m \cdot s^{-1}$. For drying air velocities greater than 1 $m \cdot s^{-1}$ some smaller particles were dragged by the air flow. In this sense, drying tests for drying air velocities greater than 1 $m \cdot s^{-1}$ were discarded. The air velocity of the centrifugal fan was controlled with a VFD (Variable

Frequency Drive) connected to an electric AC motor. Experiments were stopped when the moisture content of the sample was reduced until the equilibrium moisture content or until the samples started to burn. Furthermore, this design of experiments was used by the same authors for studying the drying of SCG-SS [24]. A comparative study will be carried out in the following sections.

2.3 Methods.

2.3.1 Mathematical models of drying curves.

Drying curves allow to see and analyse the change of moisture content in the samples with respect to time, $XR = f(t)$. Generally, drying curves are plotted from the moisture ratio which can be as (Eq. (1)):

$$XR = \frac{X_t - X_e}{X_0 - X_e} \quad (1)$$

where X_t is the moisture content at time t (dry basis), X_0 is the initial moisture content (dry basis) and X_e is the equilibrium moisture content (dry basis). However, X_e is relatively small compared to X_t and X_0 and XR can be simplified to X_t/X_0.

Drying curves were analysed for each experiment and fitted with the main mathematical models in studies on drying kinetics. In this paper, six models which present the better results of fit are used. These models are: Wang and Singh [28], Two-term Gaussian [29], Modified Page [30], the model of Midilli et al. [31], Logarithmic [32] and Two-term exponential [33]. These models are described in table 1.

Table1. Mathematical models applied to industrial spent coffee grounds drying kinetics.

Model name	Equation	Authors
Wang and Singh	$XR = 1 + at + bt^2$	Wang and Singh, 1978
Two term Gaussian	$XR = a \cdot \exp\left[-\left(\frac{t-b}{c}\right)^2\right] + d \cdot \exp\left[-\left(\frac{t-e}{f}\right)^2\right]$	Gómez-de la Cruz et al., 2014
Modified Page	$XR = \exp(-(kt)^n)$	Overhults et al., 1973
Midilli et al.	$XR = a \cdot \exp(-kt^n)$+bt	Midilli et al., 2002
Logarithmic	$XR = a \cdot \exp(-kt) + c$	Akgun and Doymaz, 2005
Two term Exponential	$XR = a \cdot \exp(-k_0 t) + c \cdot \exp(-k_1 t)$	Noomhorm and Verma, 1986

Statistical tests were utilized to find out the fit quality of the mathematical models proposed for simulating the drying data of thin layer of SCG-SCI. To verify the fit, the coefficient of determination (R^2) (Eq. (2)) and the root mean square error (RMSE) (Eq. (3)) were used.

$$R^2 = \sum_{i=1}^{N} \frac{\left(XR_{cal,i} - \overline{XR_{exp,i}}\right)^2}{\left(XR_{exp,i} - \overline{XR_{exp,i}}\right)^2} \tag{2}$$

$$RMSE = \sqrt{\frac{1}{N}\sum_{i=1}^{N}\left(XR_{exp,i} - XR_{cal,i}\right)^2} \tag{3}$$

where N is the number of data and the subscripts exp and cal mean experimental and calculated, respectively.

2.3.2 Drying rate curves.

Drying rate is a variable very important in the drying process. It represents the variation of moisture ratio with respect to time. Drying rate is crucial to optimize and

control the drying process since allows to found out the quantity of evaporated water per unit time. Drying rate can be expressed from the Eq. (4):

$$DR = -\frac{d(XR)}{dt} \approx -\frac{XR_{t+\Delta t} - XR_t}{\Delta t} \quad (4)$$

where $XR_{t+\Delta t}$ and XR_t represent the moisture content at time $t + \Delta t$ and the moisture content at time t, respectively, and t is the drying time. The minus sign is a consequence of the fact that moisture ratio decreases when the drying time increases.

Since the moisture ratio is a function of the time, experimental drying rate curves can be plotted from the moisture ratio. Furthermore, theses curves can be fitted from the derivate of the mathematical models proposed for modeling of the drying curves. Due to the drying rate is strongly dependent on the drying air temperature, the design of experiment allows for calculating this variable as function of the moisture ratio and the drying air temperature for each sample thickness, $DR = f(T, XR)$.

2.3.3 Determination of effective diffusivity.

Drying is a very complex physical process where simultaneously moisture transport and heat transfer occur. However, the great majority of drying processes of agricultural and food products take place during the falling rate period where the predominant mechanisms are the diffusion and capillary movements [22, 34]. In this sense, time-dependent effective diffusivity can be defined as an overall mass transport property which encompasses all drying phenomena. This variable can be calculated experimentally from the Fick's second law of diffusion equation:

$$\frac{\partial(\mathrm{XR})}{\partial t} = D_{eff}\frac{\partial^2(\mathrm{XR})}{\partial x^2} \tag{5}$$

where D_{eff} is the effective diffusivity ($m^2 \cdot s^{-1}$), XR is the dimensionless moisture ratio and t is the drying time (s). Dimensionless moisture ratio can be expressed from Eq. (1), described above.

The solution of the Fick's second law of diffusion equation for the one-dimensional mass transport in infinite slab geometry with uniform initial moisture distribution and negligible shrinkage is [35]:

$$XR = \frac{8}{\pi^2}\sum_{n=0}^{\infty}\frac{1}{(2n+1)^2}\exp\left(-\frac{(2n+1)^2\pi^2 D_{eff}t}{L^2}\right) \tag{6}$$

where L is the sample thickness (m). The linear solution is obtained by using a simple approach that assumes that only the first term in the series equation is significant (Eq. (7)) [36, 37].

$$XR = \frac{8}{\pi^2}\exp\left(-\frac{\pi^2 D_{eff}t}{L^2}\right) \tag{7}$$

If the natural logarithm is applied on both sides, the new equation is:

$$\ln XR = \ln\frac{8}{\pi^2} - \frac{\pi^2 D_{eff}t}{L^2} \tag{8}$$

Effective diffusivity is typically calculated by plotting the experimental drying data, as *ln XR* versus *t.* The functions *ln XR-t* in the drying of spent coffee grounds can be

fitted with linear function and, in this case, a constant value of effective diffusivity is obtained [24]. Nevertheless, experimental data were analyzed using the *modified simplified method* proposed by Gómez-de la Cruz et al. (2015) [38]. This method has been compared to the slope method [39, 40] (Eq. (9)) and several improvements like a fast calculation of this variable and an easy procedure have been proved.

$$D_{eff} = \frac{(dXR/dt)_{exp}}{(dXR/dFo)_{the}} \cdot L^2 \tag{9}$$

where Fo is the Fourier Number defined as: $Fo = \frac{D_{eff} \cdot t}{L^2}$

ln XR versus *t* can be fitted from parabolic equations. The derivate of the parabolic equations allows for obtaining the time-dependent effective diffusivity in each second as:

$$\text{slope} = \frac{\text{d}(\ln XR)}{dt} = -\frac{\pi^2 D_{eff}(t)}{L^2} \tag{10}$$

These values can be represented with respect to moisture ratio for each test, since the drying time can be replaced by the moisture ratio. Furthermore, general mathematical expressions can be obtained for calculating the effective diffusivity as a function of temperature and moisture ratio for each sample thickness.

3. Results and Discussion.

3.1 Drying kinetics analysis: drying curves and drying rates.

Dying curves were fitted with the mathematical models of the table 1. Newly, the best results of fit were obtained from the Two-term Gaussian model with an average determination coefficient of 0,999923 and an average root mean square error of 0,002435. Although this model has 6 coefficients, it has been justified due to the excellent approximation obtained in the drying rates which are, obviously, the derivate of the mathematical models [29, 37]. Table 2 reflects the quality of fit of the drying curves for each experiment from the mathematical models proposed by the table 1.

Table 2. Goodness of fit, R^2 and RMSE values, for each experiments in the drying of industrial spent coffee grounds using MATLAB.

Mathematical model	T (ºC)	Sample thickness							
		L = 5 mm		L = 10 mm		L = 15 mm		L=20 mm	
		R^2	RMSE	R^2	RMSE	R^2	RMSE	R^2	RMSE
Wang and Singh	100	0.998636	0.011203	0.998794	0.010138	0.998556	0.010673	0.996351	0.016239
	150	0.995403	0.019647	0.997605	0.014727	0.998503	0.010712	0.998039	0.012897
	200	0.994878	0.021353	0.998294	0.013440	0.998334	0.012759	0.995782	0.019211
	250	0.996189	0.020500	0.997390	0.016131	0.997315	0.015382	0.998006	0.012457
Two term Gaussian	100	0.999955	0.002232	0.999971	0.001731	0.999964	0.001839	0.999965	0.001754
	150	0.999964	0.001903	0.999988	0.001165	0.999947	0.002215	0.999985	0.001216
	200	0.999994	0.000830	0.999852	0.004339	0.999929	0.002881	0.999916	0.002964
	250	0.999937	0.002880	0.999963	0.002113	0.999449	0.007635	0.999983	0.001265
Modified Page	100	0.997353	0.015604	0.999162	0.008453	0.999673	0.005076	0.999368	0.006757
	150	0.999593	0.005843	0.999491	0.006788	0.999615	0.005432	0.999559	0.006113
	200	0.999651	0.005573	0.996868	0.018211	0.998401	0.012503	0.999315	0.007743
	250	0.999168	0.009580	0.998798	0.010946	0.998318	0.012176	0.999269	0.007543
Midilli et al.	100	0.999982	0.001341	0.999924	0.002656	0.999803	0.004121	0.999564	0.005865
	150	0.999909	0.002883	0.999897	0.003190	0.999778	0.004311	0.999722	0.005071
	200	0.999946	0.002299	0.999866	0.003928	0.999751	0.005158	0.999480	0.007043
	250	0.999636	0.006620	0.999693	0.005775	0.998885	0.010354	0.999481	0.006652
Logarithmic	100	0.999209	0.008712	0.999189	0.008493	0.999659	0.005298	0.999556	0.005789
	150	0.997795	0.013900	0.998361	0.012444	0.998736	0.010054	0.999419	0.007171
	200	0.997340	0.015719	0.998573	0.012558	0.999118	0.009482	0.999208	0.008504
	250	0.994978	0.024041	0.998028	0.014321	0.998458	0.011908	0.999014	0.008956
Two term	100	0.999280	0.008503	0.999283	0.008166	0.999678	0.005268	0.999561	0.005880
	150	0.997880	0.013936	0.998525	0.012071	0.999875	0.003236	0.999465	0.007033
	200	0.999106	0.009316	0.998681	0.012343	0.999255	0.008913	0.999228	0.008586
	250	0.995718	0.022697	0.998244	0.013819	0.998476	0.012104	0.999058	0.008962

Fig. 3 depicts the drying curves for each experiment. As can be shown, moisture ratio falls rapidly when the sample thickness decreases and the drying air temperature increases. The drying model allow predicting both the variation of moisture content and the volatile particles loss (mainly when the moisture content of the sample is low). The drying times of this waste have been compared with respect to the drying time obtained in the drying of SCG-SS. The investigations show that drying times of SCG-SCI are slightly lower for the temperatures of 200ºC and 250ºC, about 90%, regardless of the sample thickness. For the temperature of 150 ºC and 100ºC, the drying times are lower regardless of the sample thickness as well, but in these cases, the values obtained are between 65% and 75%.

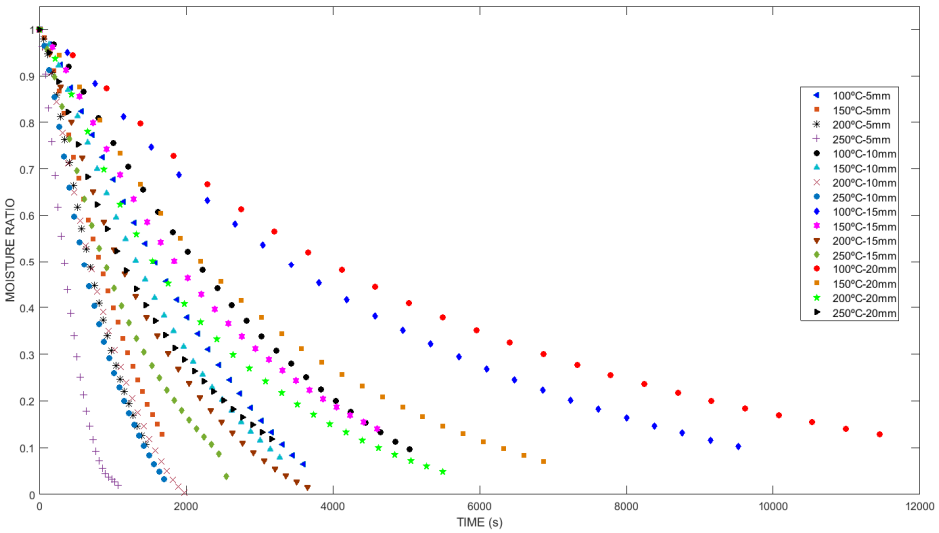

Figure 3. Drying curves at different drying air temperatures and sample thicknesses with constant air velocity, v = 1 m/s.

On the other hand, all experiments carried out at 250 ºC undergo the combustion phenomenon for moisture contents close to the equilibrium moisture content.

Furthermore, for tests performed at 200ºC and 250ºC volatile particles were released for low moisture content, < 20 % (wet basis) regardless of the sample thickness. Likewise, in contrast to the drying of SCG-SS, the SCG-SCI did not show shrinkage due to their granulometry. The sample thickness had practically the same high that at the start of the experiments. This behaviour has been observed during drying of other biomass by-products at high temperatures like olive stone [38], Hass avocado seeds [41] and mango stone [42].

Drying rate has been plotted from the moisture ratio and the drying air temperature. Fig. 4 represents these functions for each sample thickness and the drying stages can be seen: warming up period where the drying rate grows up to a maximum value (between $XR = 1$ and $XR = 0.75$), and first and second falling rate period where the drying process is characterized by diffusion pheomenon, capillary movements and sequential flow of evaporation-condensation, even release of volatile matter among other phenomena (for $XR < 0.75$). These stages have already been described by the authors in other articles [37, 38]. No constant drying rate period was appreciated during the drying experiments.

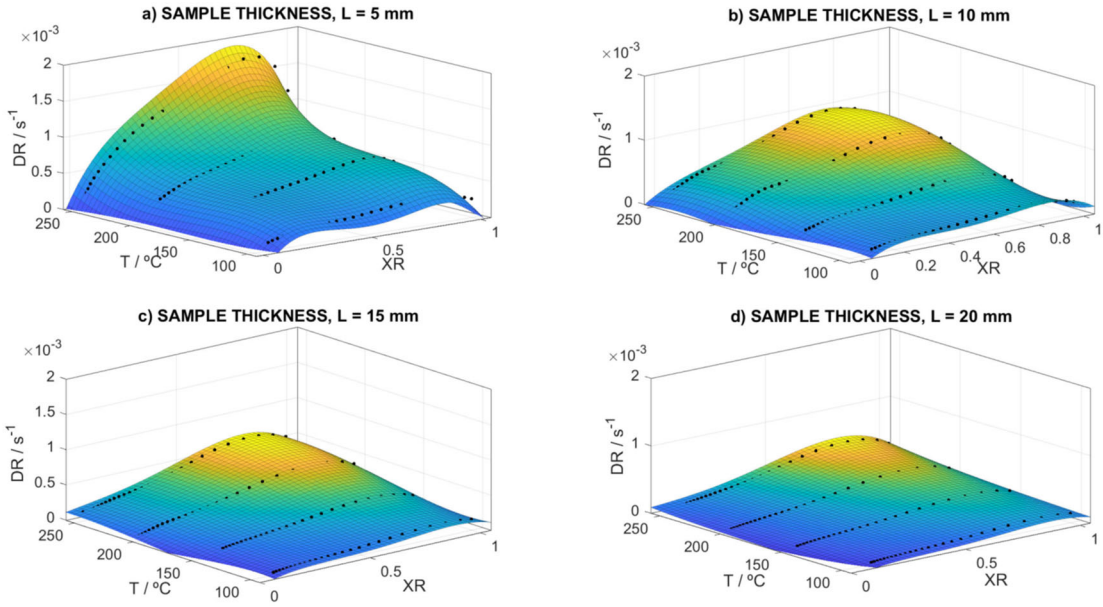

Figure 4. Drying rate surface for the sample thickness: a) L = 5 mm, b) L = 10 mm, c) L = 15 mm and d) L = 20 mm.

Fig. 4 indicates that the drying rates are higher than in the drying of SCG-SS. These values are slightly greater for sample thickness of 15 mm and 20 mm and 50% greater when the sample thickness are 5 mm and 10 mm. Drying time and drying rate in these experiments show that the drying of SCG-SCI is faster than the drying of SCG-SS. The main reason is the particle granulometry. The SCG-SS is a by-product formed mainly by powder with a particle size below 0.1 mm, whilst the SCG-SCI are formed by particles of larger size (section 2.1). It has demonstrated that when the particle size decreases the drying rate increases and the drying time diminishes due to the particle specific surface [43-45]. This phenomenon would indicate that the drying times of SCG-SS would be lower. However, the great majority of particles which form the SCG-SCI are fragments or stones of roasted coffee beans and their morphology implies that drying is more effective due to smooth non-porous surfaces.

3.2 Constant and variable effective diffusivity.

Effective diffusivity determination was calculated as a function of the time from the simplified modified method. Since the moisture ratio is obtained in function of the time, $XR = f(t)$, effective diffusivity values were expressed from the moisture ratio. Subsequently, this variable was plotted from the moisture ratio and the drying air temperature, $D_{eff} = f(T, XR)$ (fig. 5).

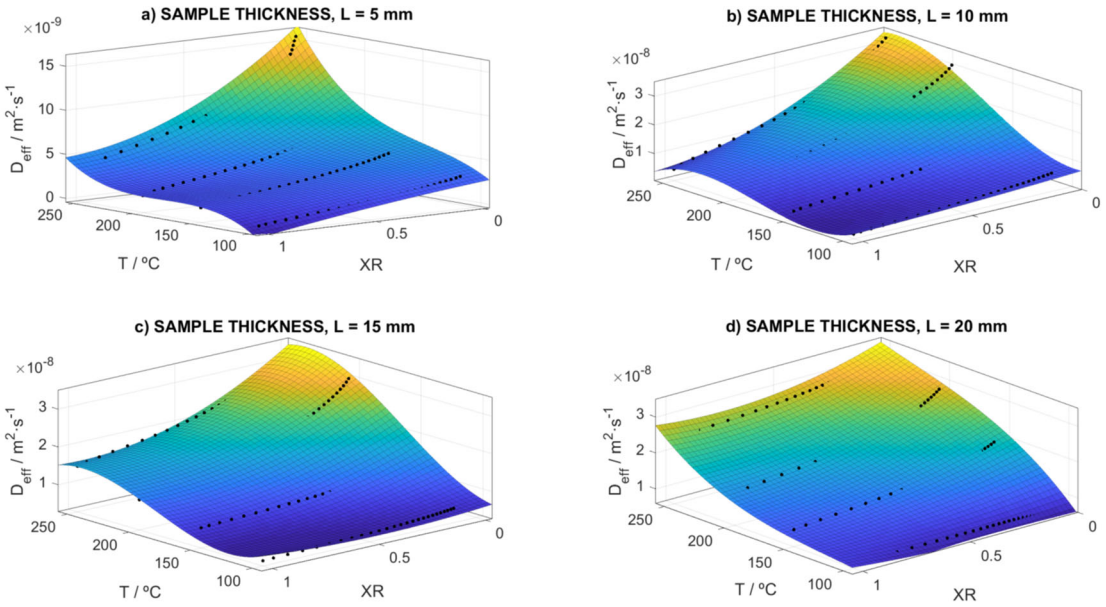

Figure 5. Effective diffusivity as a function of temperature and moisture ratio for the sample thickness: a) L = 5 mm, b) L = 10 mm, c) L = 15 mm and d) L = 20 mm.

A multiple regression analysis using the Linear Least Square allowed to fit the effective diffusivity values from a polynomial model. To define the function with a considerable quality of fit, the mathematical model proposed utilized a degree 3 for the temperature and a degree 2 for the moisture ratio with a total of 9 coefficients with 95% confidence bounds. This expression is exposed as follows bellow:

$$D_{eff} = a_0 + a_1 T + a_2 XR + a_3 T^2 + a_4 T \cdot XR + a_5 XR^2 + a_6 T^3 + a_7 T^2 XR + a_8 T \cdot XR^2 \quad (11)$$

Table 3 shows the coefficients of the mathematical model for each sample thickness y the values of R^2 and RMSE which define the goodness of fit. The effective diffusivity values were obtained for: L = 5 mm between $3.3 \cdot 10^{-10}$ m^2/s and $1.5 \cdot 10^{-8}$ m^2/s, L = 10 mm between $2.16 \cdot 10^{-9}$ m^2/s and $3.27 \cdot 10^{-8}$ m^2/s, L = 15 mm between $4.2 \cdot 10^{-9}$ m^2/s and $3.01 \cdot 10^{-8}$ m^2/s and L = 20 mm between $7.13 \cdot 10^{-9}$ m^2/s and $3.025 \cdot 10^{-8}$ m^2/s. Similar behavior can be observed during the drying of pomegranate arils [46], okra [47] and olive stone [48].

Table 3. Coefficients values of the mathematical model proposed for effective diffusivity for each sample thickness using MATLAB.

	Sample thickness / mm			
	5	10	15	20
a_0	$-1.591 \cdot 10^{-8}$	$5.508 \cdot 10^{-8}$	$3.733 \cdot 10^{-8}$	$-4.505 \cdot 10^{-8}$
a_1	$3.674 \cdot 10^{-10}$	$-1.139 \cdot 10^{-9}$	$-8.306 \cdot 10^{-10}$	$7.837 \cdot 10^{-10}$
a_2	$-1.933 \cdot 10^{-9}$	$2.034 \cdot 10^{-8}$	$2.621 \cdot 10^{-8}$	$4.289 \cdot 10^{-8}$
a_3	$-2.279 \cdot 10^{-12}$	$8.153 \cdot 10^{-12}$	$6.608 \cdot 10^{-12}$	$-2.948 \cdot 10^{-12}$
a_4	$3.077 \cdot 10^{-11}$	$-2.625 \cdot 10^{-10}$	$-3.854 \cdot 10^{-10}$	$-6.209 \cdot 10^{-10}$
a_5	$-6.116 \cdot 10^{-9}$	$-1.043 \cdot 10^{-8}$	$-3.306 \cdot 10^{-9}$	$-1.373 \cdot 10^{-9}$
a_6	$5.174e \cdot 10^{-15}$	$-1.577 \cdot 10^{-14}$	$-1.345 \cdot 10^{-14}$	$4.243 \cdot 10^{-15}$
a_7	$-3.894 \cdot 10^{-13}$	$-6.915 \cdot 10^{-14}$	$5.555 \cdot 10^{-13}$	$1.467 \cdot 10^{-12}$
a_8	$5.724 \cdot 10^{-11}$	$1.281 \cdot 10^{-10}$	$8.785 \cdot 10^{-11}$	$5.707 \cdot 10^{-11}$
R^2	0.9915	0.9922	0.9856	0.9973
$RMSE$	$3.471 \cdot 10^{-10}$	$7.73 \cdot 10^{-10}$	$1.009 \cdot 10^{-9}$	$4.291 \cdot 10^{-10}$

Experimental results reveal that as the moisture content of SCG-SCI is reduced during drying, effective diffusivity is increased. This behavior is more visible at high temperatures (200ºC and 250ºC) where the movement of water, the vapor formation and the volatile matter release is more accentuated. On the other hand, the maximum values

of effective diffusivity obtained at 250ºC are invariant of the sample thickness. Experiments carried out at 100ºC manifested that effective diffusivity practically din not depend on the moisture ratio. These phenomena can be seen in the literature, for instance during baking of white cake [49] and during the drying of olive stone [38], and similar results were found.

To perform a comparative with the values obtained in the drying of SCG-SS, constant effective diffusivity were calculated with an average value of coefficient of determination of 0.9812 (Table 4).

Table 4. Constant effective diffusivity ($m^2 \cdot s^{-1}$) of industrial spent coffee grounds during drying.

	Sample thickness / mm															
	5				10				15				20			
Temperature / ºC	100	150	200	250	100	150	200	250	100	150	200	250	100	150	200	250
D_{eff} x 10^9 / $m^2 \cdot s^{-1}$	1.79	4.06	5.85	9.46	4.57	7.62	15.3	18.9	5.38	9.85	19	22.1	7.21	15.2	21.4	29.1

Results indicate that the values found in these experiments are higher than those calculated during the drying of SCG-SS. This confirms the results obtained in the preceding sections.

4. Conclusions

Results show that drying of these wastes presents drying rate and effective diffusivity values higher than those obtained during drying of wastes generated in the services sector for the same design of experiments. The main difference is in the nature of the particles, mainly the size, which is very different in both wastes. Combustion and

volatile matter in the samples were appreciated as well. No shrinkage of the samples was found. Finally, results obtained in this research complete the studies in the drying of spent coffee grounds which will be very useful in engineering applications in several types of dryers.

Acknowledgments

This work has been conducted with the financial support of the Spanish *"Consejería Andaluza de Innovación, Ciencia y Empresa"* through the research projects AGR-6131 (*"Modelado y Control de secadero rotativo de orujo"*) and AGR-6509 (*"Producción de biocombustible utilizando hueso de aceituna y residuos de poda de olivo"*) as part of the research program *"Proyectos de Excelencia de la Junta de Andalucía 2010-2014"*. The authors gratefully acknowledge the financial support provided. The authors gratefully acknowledge to the University of Valladolid (Spain) the contribution of the industrial spent coffee grounds as well.

References

1. International Coffee Organization (ICO). Annual Review 2017/2018. 2018. http://www.ico.org/documents/cy2018-19/annual-review-2017-18-e.pdf . Accessed 10 Aug 2019.
2. Buerge IJ, Poiger T, Müller MD, Buser H. Caffeine, an anthropogenic marker for wastewater contamination of surface waters. Environ. Sci. Technol. 2003; 37:691-700. doi: 10.1021/es020125z.

3. Cruz R, Cardoso MM, Fernandes L, Oliveira M, Mendes E, Baptista P, Morais S, Casal S. Espresso coffee residues: A valuable source of unextracted compounds. J Agric Food Chem. 2012;60:7777-84. doi: 10.1021/jf3018854.
4. Morikawa CK. A new green approach to Fenton's chemistry using tea dregs and coffee grounds as raw material. Green Process Synth. 2014;3:117-25; doi: 10.1515/gps-2013-0113.
5. Muñoz Velasco P, Mendívil MA, Morales MP, Muñoz L. Eco-fired clay bricks made by adding spent coffee grounds: a sustainable way to improve buildings insulation. Mater Struct. 2016;1-2:641-50; doi: 10.1617/s11527-015-0525-6.
6. Lee HK, Park YG, Jeong T, Song YS. Green nanocomposites filled with spent coffee grounds. J Appl Polym Sci. 2015;132:42043; doi: 10.1002/app.42043.
7. Mussatto SI, Machado EMS, Martins S, Teixeira JA. Production, Composition, and Application of Coffee and Its Industrial Residues. Food Bioproc Tech. 2011; 4:661-72; doi: 10.1007/s11947-011-0565-z.
8. Kondamudi N, Mohapatra SK, Misra M. Spent coffee grounds as a versatile source of green energy. J Agric Food Chem. 2008;56:11757-60; doi: 10.1021/jf802487s.
9. Park J, Kim B, Son J, Lee JW. Solvo-thermal in situ transesterification of wet spent coffee grounds for the production of biodiesel. Bioresour Technol. 2018;249:494-500; doi: 10.1016/j.biortech.2017.10.048.
10. Todaka M, Kowhakul W. The flash points and thermal behaviors of diesel blends with biodiesels, α-pinene, d-limonene and caffeic acid as antioxidants. J Therm Anal Calor. 2019;135:2665-75; doi: 10.1007/s10973-018-7798-2.

11. Silva MA, Nebra SA, Machado Silva MJ, Sanchez CG. The use of biomass residues in the Brazilian soluble coffee industry. Biomass Bioenergy. 1998;14:457-67; doi:10.1016/S0961-9534(97)10034-4
12. Efthymiopoulos I, Hellier P, Ladommatos N, Kay A, Mills-Lamptey B. Integrated strategies for water removal and lipid extraction from coffee industry residues. Sustainable Energy Technol Assess. 2018;29:26-35; doi: 10.1016/j.seta.2018.06.016.
13. Corrêa JLG, Santos JCP, Fonseca BE, Carvalho AGS. Drying of spent coffee grounds in a cyclonic dryer. Coffee Sci. 2014;9:68-76.
14. Caetano NS, Silvaa VFM, Mata TM. Valorization of coffee grounds for biodiesel production. Chemical Engineering Transactions. 2012;26:267-72; doi: 10.3303/CET1226045.
15. Caetano NS, Silva VFM, Melo AC, Mata TM. Potential of spent coffee grounds for biodiesel production and other applications. Chemical Engineering Transactions. 2013;35:1063-8; doi: 10.3303/CET1335177.
16. Juarez GFY, Pabiloña KBC, Manlangit KBL, Go AW. Direct Dilute Acid Hydrolysis of Spent Coffee Grounds: A New Approach in Sugar and Lipid Recovery. Waste Biomass Valoris. 2018;9:235-46; doi: 10.1007/s12649-016-9813-9.
17. Sosa-Arnao JH, Nebra S. Bagasse dryer role in the energy recovery of water tube boilers. Drying Technol. 2009;27:587-94; doi:10.1080/07373930802716326.

18. Kang SB, Oh HY, Kim JJ, Choi KS. Characteristics of spent coffee ground as a fuel and combustion test in a small boiler (6.5 kW). Renew Energy. 2017;113:1208-14; doi: 10.1016/j.renene.2017.06.092.
19. Wei Y, Chen M, Li Q, Niu S, Li Y. Isothermal combustion characteristics of anthracite and spent coffee grounds briquettes. J Therm Anal Calor. 2019;136:1447-56; doi: 10.1007/s10973-018-7790-x.
20. Casanova-Peláez PJ, Palomar-Carnicero JM, Manzano-Agugliaro F, Cruz-Peragón F. Olive cake improvement for bioenergy: the drying kinetics. Int J Green Energy. 2015;12:559-69; doi:10.1080/15435075.2014.880347.
21. Strumillo C, Kudra T. Drying: Principles, application and design. London, Great Britain: Gordon and Breach; 1986.
22. Vasić M, Grbavčić Ž, Radojević Z. Analysis of Moisture Transfer During the Drying of Clay Tiles with Particular Reference to an Estimation of the Time-Dependent Effective Diffusivity. Drying Technol. 2014;32:829-40; doi:10.1080/07373937.2013.870194.
23. Efremov G, Kudra T. Calculation of the effective diffusion coefficients by applying a quasi-stationary equation for drying kinetics. Drying Technol. 2004;22:2273-9; doi: 10.1081/DRT-200039993.
24. Gómez-de la Cruz, F. J., Cruz-Peragón F, Casanova-Peláez PJ, Palomar-Carnicero JM. A vital stage in the large-scale production of biofuels from spent coffee grounds: The drying kinetics. Fuel Process Technol. 2015;130:188-96; doi: 10.1016/j.fuproc.2014.10.012.

25. Hussain MM, Dincer I. Two-dimensional heat and moisture transfer analysis of a cylindrical moist object subjected to drying: a finite-difference approach. Int J Heat Mass Transfer. 2003;46:4033-9; doi: 10.1016/S0017-9310(03)00229-1.
26. Kaya A, Aydın O, Dincer I. Numerical modeling of heat and mass transfer during forced convection drying of rectangular moist objects. Int J Heat Mass Transfer. 2006;49:3094-103; doi: 10.1016/j.ijheatmasstransfer.2006.01.043.
27. Wang CY, Singh RP. Use of variable equilibrium moisture content in modeling rice drying. Transaction ASAE 1978;11:668-72.
28. Gómez-de la Cruz, F. J., Casanova-Peláez PJ, Palomar-Carnicero JM, Cruz-Peragón F. Drying kinetics of olive stone: a valuable source of biomass obtained in the olive oil extraction. Energy. 2014;75:146-52; doi: 10.1016/j.energy.2014.06.085.
29. Overhults DG, White GM, Hamilton HE, Ross IJ. Drying of soybeans with heated air. Transactions ASAE 1973;16:112-3.
30. Midilli A, Kucuk H, Yapar Z. A new model for single-layer drying. Drying Technol. 2002;20:1503-13; doi:10.1081/DRT-120005864.
31. Akgun NA, Doymaz I. Modelling of olive cake thin-layer drying process. J Food Eng. 2005;68:455-61; doi: 10.1016/j.jfoodeng.2004.06.023.
32. Noomhorm A, Verma LR. Generalized single-layer rice drying models. Transactions ASAE 1986; 29:587-591.
33. Pathare PB, Sharma GP. Effective moisture diffusivity of onion slices undergoing infrared convective drying. Biosyst Eng. 2006;93:285-91; doi: 10.1016/j.biosystemseng.2005.12.010.

34. Crank J. The mathematics of diffusion. . Oxford, England: Clarendon Press; 1975.
35. Li H, Chang Q, Gao R, Dai Z, Chen X, Yu G, Wang F. Thin-layer drying characteristics and modeling of lignite under supercritical carbon dioxide extraction and the evolution of pore structure and reactivity. Fuel Process Technol. 2018;170:1-12; doi: 10.1016/j.fuproc.2017.09.010.
36. Gómez-de la Cruz, Francisco J, Casanova-Peláez PJ, López-García R, Cruz-Peragón F. Review of the Drying Kinetics of Olive Oil Mill Wastes: Biomass Recovery. 2015;10:6055-80; doi:10.15376/biores.10.3.Cruz.
37. Gómez-De La Cruz, F. J., Palomar-Carnicero JM, Casanova-Peláez PJ, Cruz-Peragón F. Experimental determination of effective moisture diffusivity during the drying of clean olive stone: Dependence of temperature, moisture content and sample thickness. Fuel Process Technol. 2015;137:320-6; doi: 10.1016/j.fuproc.2015.03.018.
38. Pinto L, Tobinaga S. Diffusive model with shrinkage in the thin-layer drying of fish muscles. Drying Technol. 2006;24:509-16; doi:10.1080/07373930600612040.
39. Babalis SJ, Belessiotis VG. Influence of the drying conditions on the drying constants and moisture diffusivity during the thin-layer drying of figs. J Food Eng. 2004;65:449-58; doi: 10.1016/j.jfoodeng.2004.02.005.
40. Avhad MR, Marchetti JM. Mathematical modelling of the drying kinetics of Hass avocado seeds. Ind Crops Prod. 2016;91:76-87; doi: 10.1016/j.indcrop.2016.06.035.

41. Wilkins R, Brusey J, Gaura E. Modelling uncontrolled solar drying of mango waste. J Food Eng. 2018;237:44-51; doi: 10.1016/j.jfoodeng.2018.05.012.
42. Gómez-De La Cruz, F. J., Casanova-Peláez PJ, Palomar-Carnicero JM, Cruz-Peragón F. Modeling of olive-oil mill waste rotary dryers: Green energy recovery systems. Appl Therm Eng. 2015;80:362-73; doi: 10.1016/j.applthermaleng.2015.01.035.
43. Arjona R, García A, Ollero P. Drying of alpeorujo, a waste product of the olive oil mill industry. J Food Eng. 1999;41:229-34; doi: 10.1016/S0260-8774(99)00104-1.
44. Gögüs F, Maskan M. Air drying characteristics of solid waste (pomace) of olive oil processing. J Food Eng. 2006;72:378-82; doi: 10.1016/j.jfoodeng.2004.12.018.
45. Dak M, Pareek NK. Effective moisture diffusivity of pomegranate arils under going microwave-vacuum drying. J Food Eng. 2014;122:117-21; doi: 10.1016/j.jfoodeng.2013.08.040.
46. Dadali G, Apar DK, Özbek B. Estimation of effective moisture diffusivity of okra for microwave drying. Dry Technol. 2007;25:1441-6; doi: 10.1080/07373930701536767.
47. Cuevas M, Martínez-Cartas ML, Pérez-Villarejo L, Hernández L, García-Martín JF, Sánchez S. Drying kinetics and effective water diffusivities in olive stone and olive-tree pruning. 2019;132:911-20; doi: 10.1016/j.renene.2018.08.053.
48. Sakin M, Kaymak-Ertekin F, Ilicali C. Modeling the moisture transfer during baking of white cake. J Food Eng. 2007;80:822-31; doi: 10.1016/j.jfoodeng.2006.07.011.